

MOBILITY AND CONDUCTIVITY OF IONS IN AND INTO POLYMERIC SOLIDS

R. EDWARD BARKER, JR

Department of Materials Science, School of Engineering and Applied Science, University of Virginia,
Charlottesville, VA 22903, USA

Abstract—There often has been great uncertainty as to whether typical measurements allow one to conclude that conduction in a given polymer is due predominately to ions or to electrons. Many researchers have assumed that relatively pure polymers can be treated as wide band gap semi-conductors but other scientists have believed that most non-conjugated polymers conduct by the movement of ions. Part of the trouble is that many of the theories predict dependences of current on voltage and sample thickness too similar to easily distinguish between the assumed mechanisms unless extensive and very good data are available. Some comparisons are discussed. More recent approaches that use pressure as an added variable, or those that give careful consideration to such things as gas evolution often allow one to deduce the predominant type of conduction. The concept of local structure of a polymer in the neighborhood of an ion is considered along with the relation of ionic conduction to the entropy correlation theory recently developed by Barker and applied to the case of diffusion in oriented polymers by Barker, Tsai, and Willency. According to the evidence, the activation entropy increases under the action of an organizing effect such as uniaxial elongation.

Moisture has two important effects on conduction in polymers. At low concentrations it contributes charge carriers by its own dissociation and at higher concentrations it enhances the dissociation of other ionic species present. Some data for the correlation of conductivity and dielectric constant of solid polymers are discussed in terms of the weak electrolyte model developed by Sharbaugh and Barker for organic liquids. The existence of the correlation seems to imply that many polymers, under most circumstances, are predominantly ionic conductors.

1. INTRODUCTION

Even today it remains surprisingly difficult to unambiguously determine all of the important features of electrical conduction in polymers. This is in part due to the fact that several of the solid state theories that have been useful in establishing the properties of crystalline semi-conductors and insulators give predictions that are not sufficiently unique when applied to data for polymers. Another very real source of difficulty is the great morphological complexity of most polymeric systems. The people who study dielectric relaxation seem to be well aware of the various structural features, for example when they distinguish between α_c relaxations in the crystalline regions and α_a losses in the amorphous portions, however there has been some inclination, particularly among workers making direct current (dc) measurements, to view the motion of an ion to take place in a dielectric continuum. Although certain types of continuum models still have a useful place, future progress depends on accounting for the effects of internal structure on the conduction process. One of the purposes of this paper is to discuss what will be called the local structure hypothesis, by which I mean that a given ion not only is very much influenced by the various structural features of the polymer, it also modifies them in its own local neighborhood and therefore probes what may be a temporarily atypical part of the polymer. Some other interrelated purposes are to discuss some of the techniques for trying to decide whether conduction is due to ions or to electronic mechanisms and to comment on the processes whereby ions enter a polymer. A schematic view of ions in a polymer is shown in Fig. 1.

2. NATURE OF THE CONDUCTION PROCESS IN POLYMERS

In polymers as a class of materials both electrons and ions contribute to the total conductivity, however in a

given case it is likely that one type of conductivity will predominate. As the intensive variables of the system are changed, it is conceivable that the predominant mode will shift to another type. As illustrated in Table 1, the electronic and ionic contributions can be subdivided into several categories. For electronic conduction, either electrons or holes may be the majority carrier and the process may be either intrinsic, a property of a pure material such as silicon, or extrinsic, depending upon trace impurities to obtain a high level of conductivity, as in the case of silicon doped with arsenic or phosphorous.¹ Analogously, although the detailed mechanisms are quite different, ionic conductivity can be intrinsic or extrinsic in the sense of impurities, and the total current may be due predominantly to mobile cations, as in the case of the sodium salt of poly(methacrylic acid), or to mobile anions, as for secondary amine derivatives of polystyrene. Mark² recently described the general features of a new polyelectrolyte membrane developed in Australia that allows its counter ions to be removed thermally without the need for additional chemicals. This broadens the analogy with the electronic processes. In polymers such as the polyolefins, -alkyl methacrylates, -carbonates and many others that do not have easily ionizable groups, such as OH, it often is considered plausible that conduction depends upon being able to inject electrons (or holes) into the material at the electrodes, or perhaps into the bulk by irradiation, and thus that the conduction process must surely be electronic. In many cases when this argument is offered in conjunction with data for a particular polymer under very well controlled and specified conditions the conduction may in fact be electronic but the argument more often suffers from the fact that the measurements were made in air of moderate humidity (even ASTM D257 specifies conditioning samples in standard humidity conditions). Most organic polymers sorb significant amounts of all low molecular weight gas and vapor

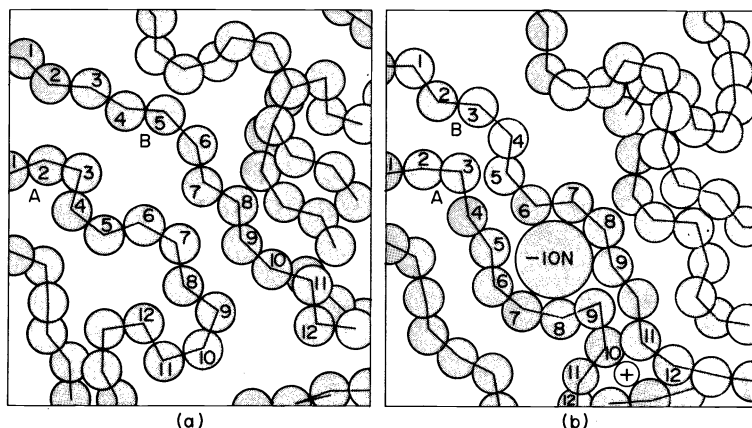


Fig. 1. Schematic representation of chains in a non-crystalline polymer. In (a) note the chains A and B when no ions are present. In (b) an ion pair has reduced the number of configurations available to A and B.

Table 1. Modes of conduction in polymers

I. Electronic	
1.	Conduction by electrons (<i>n</i> -type)
(a)	Intrinsic
(b)	Extrinsic (impurities donate electrons)
2.	Conduction by holes
(a)	Intrinsic
(b)	Extrinsic (impurities accept electrons)
3.	Metallic type conduction
	Rare in polymers; polythiazyl $(-SN-)_n$ is one example†
II. Ionic	
1.	Electrolytic (cationic, anionic, ambipolar)
(a)	Intrinsic (self dissociating)
(b)	Extrin (impurities or dopants)
2.	Protonic
	e.g. in Nylon 66 and poly(ethylene oxide)

†cf. M. M. Labes, Ref. 49.

molecules. For example measurements by Norton³ show that polycarbonate, which is thought of as having a relatively low degree of moisture uptake, has a sorption coefficient of 169 std-cc/atm cc or 6.6×10^{19} water molecules/cm³ at 50% relative humidity. Norton's value for the oxygen in polycarbonate for normal ambient conditions is 2.9×10^{18} molecules/cm³. His values for the diffusion coefficients are $D(\text{H}_2\text{O}) = 6.8 \times 10^{-8}$ cm²/sec ($\times 10^{-12}$ m²/sec), and $D(\text{O}_2) = 2.1 \times 10^{-8}$ cm²/sec. These data which are representative for non-polar polymers can be utilized to place the interpretation of electrical conductivity data in an interesting perspective.

A. Ionic conduction that appears to be electronic

The argument that conduction must be electronic in polymers whose chemical structure contain no easily ionizable groups tends to ignore the gases dissolved in the sample. Consider the situation in terms of the following model for conduction. Assume that an oxygen molecule diffuses to the cathode, where due to its moderate electron affinity it becomes a negative ion. Then under the action of the electric field *E*, its diffusive pathway will be biased toward the anode which it will reach after a time given by

$$t_E = b/uE = b^2/uV, \quad (1)$$

†Possible short comings of the NET relation will be discussed later.

where *b* is the distance between the electrodes and *u* is the effective ionic mobility of O_2^- . At the anode it will deposit the electron, become a neutral molecule again and thus be able to carry out this shuttle operation any number of times. As far as the external circuitry is concerned it might appear that the electron had traveled directly through the polymer. To see if this model is reasonable, it is necessary to estimate *u* and the average time *t* needed for the diffusion and charge transport cycle. It would be interesting to solve the set of diffusion and kinetic equations appropriate to the model but for present purposes it is felt that the following simple argument based on dimensional considerations is quite adequate. The time *t* consists of three parts, a time t_D for diffusion, t_E for the movement of the ion, and a time t_R during which the ion resides on trapping sites. If *u* is the effective mobility then t_R is already accounted for but in any event it seems unlikely that t_R will exceed t_D . Thus, including t_R in t_E we have $t = t_D + t_E$ so that a current per ion i_1 can be defined by the equation

$$i_1 = e/(t_D + t_E) = e/[(b^2/D) + (kTb/eD)] \quad (2)$$

where, in addition to eqn (1), an upper limit for the time for diffusion is approximated by

$$t_D = b^2/D, \quad (3)$$

and the Nernst-Einstein-Townsend (NET) relation

$$ukT = eD \quad (4)$$

is utilized to obtain an estimate of *u* from *D*.† For illustrative purposes consider a 1 mm-thick sample between parallel plane electrodes at *V* = 1000 volt potential difference and at *T* = 300 K. By the use of Norton's³ values for $D(\text{O}_2)$, in polycarbonate, in eqn (3), and then in eqns (4) and (1), one gets

$$t_D = 5 \times 10^5 \text{ sec}, \quad u = 7.7 \times 10^{-11} \text{ m}^2/\text{V} \cdot \text{sec},$$

and $t_E = 12 \text{ sec}.$

As one could have easily anticipated the process is strongly diffusion limited because $t_D \gg t_E$. The current per ion is thus

$$i_1 \approx 1.6(10^{-19} \text{ C})/5(10^5 \text{ sec}) \approx 3(10^{-25} \text{ A}).$$

It can be noted that the current density j is given by

$$j = nbi_1 = n_0fb_1 \quad (5)$$

where $n = n_0f$, n_0 is the concentration of oxygen, and f is the fraction that has become negatively charged. Now the usual definition of conductivity, $\sigma = j/E$, leads to

$$\dot{\sigma} = n_0fb_1/E = n_0b^2i_1f/V. \quad (6)$$

Use of the previous values gives

$$j \approx (9 \times 10^{-4} \text{ Am}^{-2})f \quad \text{and} \quad \sigma \approx (9 \times 10^{-10} f) \text{ rom.}^\dagger$$

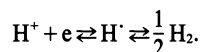
What the simple model illustrates is that, if f is assigned any value between 10^{-6} and 1, the contribution to a sample's conduction due to oxygen diffusion is significant. Presumably the nature of the polymer and electrodes would influence f , the fraction of oxygen negative ions, and certainly one would expect f to depend on the field intensity E_c at the cathode. The role of water in the conduction processes will be discussed in section III-E.

B. Protonic conduction

In a few polymers a rather special kind of conduction process occurs which may be called protonic conduction. Some excellent studies of this process have been made by Binks and Sharples⁴ for olefin oxide polymers and by Seanor⁵ for nylon 66. The olefin oxide polymers behave in a surprising way. Due to the facts that they contain no unsaturated bonds and are relatively hydrophobic, one would expect them to be rather typical polymeric insulators with $\sigma \sim 10^{-15}$ rom. Indeed, the first member of the series, polymethylene oxide ($-\text{CH}_2\text{O}-$), does have the expected magnitude of conductivity, but poly-(ethylene oxide), -(trimethylene oxide), and -(tetramethylene oxide) have conductivities that are larger by six to nine decades. A series of careful experiments showed that atmospheric water accounted for about 2/3 of a decade change and that the effects of O_2 and N_2 were much smaller. Therefore they concluded that the large increase in σ was an intrinsic property. The mechanism they proposed appears to be a very reasonable one. The idea is that a proton will be removed from one of the methylene groups adjacent to an ether oxygen and attached to another ether oxygen on a close-by chain segment, where it will remain until the segment rotates to come into a position favorable for transfer of the proton to another oxygen. Thus in the presence of an external field, these protons will be able to migrate from one ether oxygen to another down field if there is sufficient segmental mobility to bring the groups into the proper relative positions for proton transfer to occur. Eley and Spivey⁶ have proposed a somewhat similar mechanism for the polyamides. It is thought that the much lower conductivity of PMO relative to that for PEO, (and higher members of the methylene oxide series) is due to its much lower segmental mobility at 25°C. The glass transition T_g of PMO is 280°K whereas it is only 215°K for PEO.

In his study of nylon 66, Seanor⁵ addressed one of the central but often over looked issues in the dilemma between ionic and electronic conduction: namely, is there mass transport proportional to the charge transport? He observed three temperature regions: (I) below 80°C, (II)

between 80 and 110°C, and (III) near and above 120°C. In the lowest region the conduction decreased over a long time but there was negligible gas evolution. In the middle region there was slight gas evolution and the current remained relatively constant, whereas in the highest temperature region, a continuous decrease in σ was observed and there was enough H_2 gas evolution to account for half of the charge transfer on the assumption of a protonic conduction process. Seanor's conclusion was that conduction in the high temperature region involved both electrons and protons but that below 110°C it was mainly electronic. However if the O_2 -shuttle mechanism (or some similar process) were in operation one could have ionic conduction without the expected net mass transfer. A number of other workers including King and Medley,⁷ Murphy,⁸ and Binks and Sharples⁴ have also detected mass transfer in various polymers. In fact Binks and Sharples⁴ made the important observation that after a long term conductivity measurement, there was a reverse voltage of 1.7 V (independent of the original polarizing voltage) which upon shorting could provide a current density of over 3×10^{-10} A/cm² for a long time in 0.5 mm thick samples. The reverse voltage of 1.7 V supports strongly the hypothesis of recombination of atomic hydrogen at their silver paste electrode to create an electrochemical cell.



C. Spontaneous voltages and currents in metal-polymer-metal systems (MPMS)

The work of Binks and Sharples⁴ suggested that proton concentrations, near the electrodes, produced by an applied field could subsequently lead to specific reverse voltages of electrochemical origin. In a recent interesting study by Ieda *et al.*⁹ measurements were made of the open circuit voltage (with a $10^{13} \Omega$ vibrating reed electrometer) across 25 μm thick poly(ethylene terephthalate) sandwiched between two different vacuum-deposited metals. The short circuit currents also were measured at several temperatures. Seven metals and eleven combinations were used so their work is significant in its scope. The measured open circuit voltage V_0 increased rapidly, from virtually zero, as temperatures rose above 80–90°C and reached a maximum at about 120°C. Thereafter, V_0 appears to decrease very slowly. The values of V_0 at 120°C are given in Table 2. The short circuit currents of 10^{-13} – 10^{-10} A/cm² appeared to give linear Arrhenius plots with activation energies between 1.7 and 2.0 eV. Unfortunately it was not easy to deduce the individual activation energies from their graph. A major implication of the work by Ieda *et al.*⁹ is that the $\text{M}_1/\text{PET}/\text{M}_2$ structure constitutes a galvanic cell with electrode reactions to supply the energy to drive the current. It would not be expected that the contact potential differences could maintain a sustained current such as was observed. The details of the chemical reactions have not yet been established. It would appear to be very useful to have additional data of the kind obtained but in a variety of controlled atmospheres and also to have data for decreasing as well as increasing temperature.

Conduction in PET has been widely studied^{10–20} but there is a relatively even division between those^{10–15} who attribute its conductivity to ions and those^{16–20} who ascribe it to electronic processes. Probably both types of conductivity are involved with the ionic mechanisms

[†]For convenience, the notation rom = reciprocal-ohm-meter is used.

Table 2. Open circuit voltages for M_1 /PET/ M_2 structures†

	$M_1(+)$	$M_2(-)$	V_0 [volt]‡
1	Au	Al	(1.3)§
2	Al	Pb	0.70
3	Sn	Au	0.55
4	Zn	Au	0.55
5	Ag	Pb	0.48
6	Cu	Pb	0.40
7	Ag	Au	(-0.33)¶
8	Pb	Au	0.23
9	Cu	Au	0.06
10	Pb	Zn	0.055
11	Pb	Sn	0.056

†Based on data of Ieda *et al.*⁹ V_0 was much smaller when M_1 and M_2 were the same metal.

‡Peak value, after heating at 0.67°C/min.

§Their graph indicates 1.3 V but their table gave 1.05 V.

¶Only this pair exhibited a polarity opposite to what would be expected from the electromotive series.

predominating at lower fields and higher temperatures, and electronic processes making a greater contribution at higher fields.^{9,15}

D. Limitations on the Nernst-Einstein-Townsend relation

The NET equation $ukT = zeD$ is extremely useful. A great deal is known about diffusion in polymers as a function of the size and nature of the diffusant molecules and the nature and condition of the polymer. Thus to the extent that the NET relation is valid we can predict much of the behavior of the mobility u of an ion if we can match it with an appropriate gas molecule whose diffusion in the polymer of interest has been measured. For example since a typical gas molecule of 3 Å diameter might have a diffusion coefficient $D(300^\circ\text{K}) \sim 10^{-12} \text{ m}^2/\text{sec}$, the NET relation predicts that an ion of the same *effective* size should have

$$u(300^\circ\text{K}) \sim 40 D \quad (7)$$

or about $4 \times 10^{-11} \text{ m}^2/\text{V} \cdot \text{sec}$ ($4 \times 10^{-7} \text{ cm}^2/\text{V} \cdot \text{sec}$).

If the origin of the NET relation is recalled some of its limitations become apparent. It can be derived by assuming two things: (1) a balance ($j_E + j_D = 0$) of the current density

$$j_E = \sigma E = unqE \quad (8)$$

of a single type of charge carrier q in an applied field E , against a back diffusion term

$$j_D = -qD(\partial n/\partial x), \quad (9)$$

and (2) an assumed Boltzmann distribution

$$n = n_0 \exp(-Vq/kT) \quad (10)$$

of the charge carriers, for the potential $V = V(x)$. When more than one mobile charge carrier is involved there should be current densities $j_E(i)$ and $j_D(i)$ for each of the ion densities $n(i)$. For example if there are two types of charge carriers (e.g. Na^+ and Cl^-), then instead of the

NET equation, the Nernst-Hartley (or ambipolar diffusion) relation is supposed to be better. The Nernst-Hartley relation involves the following assumptions²⁰

$$j_E = j_E^+ + j_E^- \quad \text{and} \quad j_D = j_D^+ + j_D^-$$

$$j = j_E + j_D = (u^+n^+q^+ - u^-n^-q^-)E - q^+D^+\left(\frac{\partial n^+}{\partial x}\right) - q^-D^-\left(\frac{\partial n^-}{\partial x}\right). \quad (11)$$

For electroneutrality $n^+q^+ = n^-q^-$ with $q^+ = z^+e$ and $q^- = -z^-e$, the result can be expressed

$$D_{\text{effective}} = \frac{kT(1/z)_{\text{eff}}}{e(1/u)_{\text{eff}}} = \frac{kT}{e} \left(\frac{1}{z^+} + \frac{1}{z^-} \right) \left(\frac{u_+u_-}{u_+ + u_-} \right) \quad (12)$$

which is a version of the Nernst-Hartley equation. Actually, as discussed by Robinson and Stokes,² there is an extra small factor on the right side, that involves the activity coefficients of the ions. For most of the purposes in the present paper the NET relation will be used but there is another kind of difficulty. Namely, in what way does the diffusion coefficient D_i of an ion differ from that of a neutral molecule of the same size? The point of view in the present paper is that the ion should have a smaller diffusion coefficient than the molecule but there is at least some evidence that this may not be true. For example, Foss and Dannhauser^{21,22} and Kallweit²³ have shown that the effective viscosity experienced by an ion moving in a polymer is less than one would expect the macroscopic viscosity to be.

3. THE LOCAL STRUCTURE HYPOTHESIS

A. Basis for the hypothesis

As implied earlier, by virtue of their low concentration and because of their electrostatic interaction with the surrounding material, ions may probe regions of a polymer that are atypical of the sample as a whole. For example, Barker and Thomas²⁴ have presented evidence that, in the case of cellulose 2.5 acetate of bulk modulus B , the value of the glass transition temperatures determined by conductivity measurements depend upon the types of conducting ions. The shift in T_g was found to be predictable from the well known statistical mechanical relation,

$$\langle (V - V_0)^2 \rangle_{\text{avg}} = kTV_0/B, \quad (13)$$

for the fluctuation of the volume V of a fixed number of particles after the additional stipulation that an effective ionic interaction volume, mW_i , should be subtracted from the instantaneous volume V of the group of molecular units participating in a unit diffusional process (i.e. the cooperative motion that must occur for the ion to move to a site outside of the group). The physical interpretation is that the ion reduces the local free volume and thus raises the local T_g . For an ideal crystal, impurities will introduce disorder and thus cause a lowering of the melting point but for a glassy polymer which already has a large amount of disorder, an ion can produce an increase in the local order and thus an increase in T_g . It must be emphasized that for the cases discussed, the ions occupy a small volume fraction of the total sample and thus they will not produce a significant change in T_g as measured dilatometrically or mechanically. The equation of Barker and

Thomas²⁴ for the change in T_g is a quadratic in ion volume W_i , i.e.

$$\Delta T_g = -2 am\delta \cdot W_i + am^2 W_i^2 \quad (14)$$

δ is a measure of free volume, a is determined by the bulk modulus of the polymer and the size of the activated molecular cluster about the ion, and m is a measure of the ion's interaction size relative to its geometric size.

B. Range of ionic interaction

To obtain an improved perception of the relative range of interaction of an ion with its surroundings consider the Coulombic interaction energy U_{ij} between two ions i and j with a distance $r_{ij} = r_i + r_j$ between centers. With energy in [eV] and distance in [Å], the equation for z -valent ions is,

$$U_{ij} = 14.4 z_i z_j / \kappa r_{ij} \quad (15)$$

where κ is the effective static dielectric constant of the medium. The form of this equation is so well known and simple that it is not usually plotted but for understanding the behavior of ions in polymers it is really quite instructive to do so. Figure 2 shows a log-log plot of eqn (15) for several typical values of κ . Horizontal dashed lines give reference values of kT at a number of temperatures. One deficiency of this approach is that the medium is treated as a homogeneous infinitely divisible dielectric, with κ independent of E , nevertheless, it can be seen that our main interest will be with three regions: A, B, and C. For typical bare ions, area A would be the region of interest. (In a vacuum A would be moved up to $\kappa = 1$.) If hydration or other solvation is involved, as will often be the case, then region B is the one of most concern. Thus ions in a polymer, as indicated by region B,

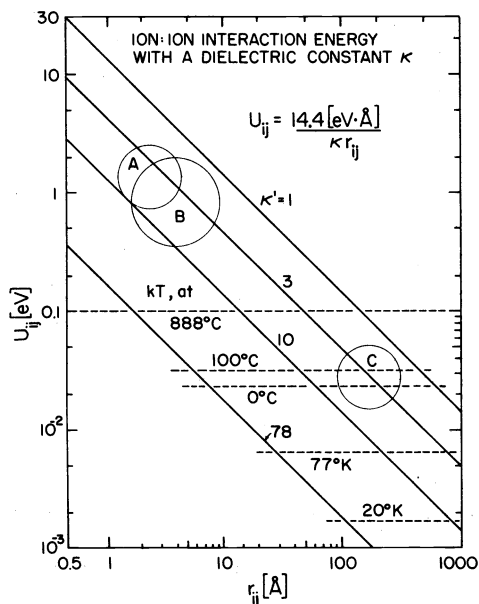


Fig. 2. Coulombic interaction energy between monovalent ions separated by a distance r_{ij} in media of different dielectric constant. The horizontal dashed lines indicate values of kT at several temperatures. The circles are only schematic to locate areas of special interest: A—close approach of bare ions, B—hydrated or solvated ions, and C—the several hundred Å domain in which the ions electrostatic energy exceeds kT .

will have about 1 eV of Coulombic attractive energy but the same ion pair in water would only have 0.05 eV. Thus as Sharbaugh and Barker^{25,26} discussed previously, substances that are normally thought of as strong electrolytes will behave as weak electrolytes in a low dielectric constant polymer. On the other hand, the fractional dissociation ϕ of a given salt in a polymer of dielectric constant 10 or even 3 is going to be vastly larger than for the same salt in a vacuum. Another portion of this plot that is of great interest is region C. Note that whereas regions A and B were concerned with ions in their closest proximity, region C corresponds, for typical polymers, to the size domain in which ionic attraction (or repulsion) exceeds the effect of thermal agitation. The domain is surprisingly large, being hundreds of Ångströms in diameter. The effective radius of such a domain for monovalent ions is given by

$$r_D \sim K e^2 / \kappa kT \sim 555 \text{ Å} / \kappa \quad (16)$$

at 300°K (K is 9×10^9 SI units.)

From a slightly different point of view the local electric field intensity about an ion is the best measure of its influence. The relation between the field and the distance from the ion is shown in Fig. 3 for the same four values of the dielectric constant. The equation

$$r = 3.794 \times 10^5 / \sqrt{\kappa E} \quad (17)$$

is merely $E = e/4\pi\epsilon_0\kappa r^2$ solved for r in [Å] when E is in [V/m]. The idea here is that if one chooses a certain external applied field, say $E_a = 10^5$ V/m positive toward the right for example, then the distance on the left side of the ion at which the resultant of the two fields is zero can be read from the graph. In this example it is about 700 Å for a polymer with a dielectric constant of 3. Of course on the right side of the ion at a distance of 700 Å the fields add to give about 2×10^5 V/m there. The important thing is that an ion's field dominates in the polymeric material throughout a region with a diameter of over 1000 Å for the example. In fact the applied field would have to be 10^{10} V/m to reduce the ion's range of dominance to about 3 Å. For typical values of applied fields used in many electrical measurements it is apparent that the range of dominance of an ion's field extends over several million mers and could encompass small crystallites and other intermediate scale morphological features.

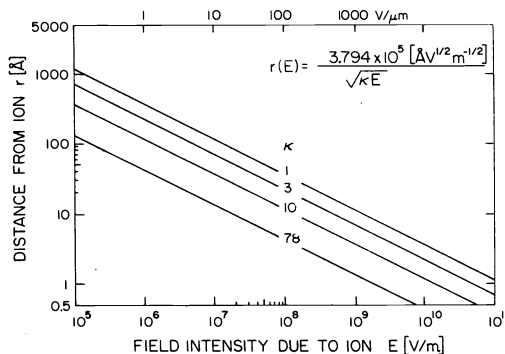


Fig. 3. Distance from a monovalent ion corresponding to a given field strength E . These curves give the range at which the ion's field will cancel the opposing component, E , of an applied field. For fields of the "kV/cm" magnitude, the range is hundreds of Ångströms and is thus comparable with the "jump distances" of rate theory.

C. Interaction with interfaces

Due to the supramolecular extent of the ion's interaction range it will be expected to interact with the interfaces between crystalline and amorphous regions. Crystalline regions will have a slightly greater dielectric constant κ_c than that κ_a of the amorphous regions. A simple model will now be developed to predict the interaction. A consequence of the model is that the interaction provides attractive trapping forces such that thermal detrapping might give current pulses at reasonably well defined temperatures.

Consider an ion deep in the interior of a typical semiamorphous and non-oriented polymer. At a distance of say a million ionic diameters away, the material should appear fairly homogeneous and isotropic to a hypothetical observer on the ion. However as a point closer to the ion is considered, say less than 1000 diameters then the inhomogeneities will begin to be noticeable. How will the ion interact with these inhomogeneous features of the material? Perhaps the easiest way to get a feeling for this is to consider two simple models: a planar inhomogeneity and a spherical one. It will be imagined temporarily that the rest of the sample is homogeneous.

The planar inhomogeneity is analogous to close range interaction with a polymer crystallite. For explicitness it is assumed that the ion is in the non-crystalline part of the sample.

From elementary electrostatic theory, it can be seen that there is an attractive force between the ion and the crystallite, along the normal to the interface. For a metallic interface, the electric field lines would at every point be perpendicular to the planar interface with the result that the image charge would be of the same size and opposite sign to the ion's charge. However, for a planar interface between dielectrics the field lines bend abruptly with normal angles given by²⁷

$$\tan \alpha_c / \tan \alpha_a = \epsilon_c / \epsilon_a = \kappa_c / \kappa_a \quad (18)$$

and the image charge Q' is given by

$$-Q' = \frac{\epsilon_c - \epsilon_a}{\epsilon_c + \epsilon_a} Q = \frac{\kappa_c - \kappa_a}{\kappa_c + \kappa_a} Q \quad (19)$$

which appears to be located (so far as the non crystalline region is concerned) at the same depth x below the interface as the real charge is above it. The permittivity of the crystalline region ϵ_c exceeds that of non crystalline region ϵ_a so Q' has the opposite sign to Q . A relation between the density, or number of molecular groups per unit volume is provided by the Clausius-Mossotti relation:

$$\frac{\kappa - 1}{\kappa + 2} = \sum \frac{N_i \alpha_i}{3} \text{ (SI-units); } \sum \frac{4}{3} \pi N_i \alpha_i \text{ (cgs-units).} \quad (20)$$

The sum is over the products of the number N_i in unit volume of each type of polarizable group and the

corresponding polarizability α_i . Some representative values of bond polarizabilities, which are approximately additive, are given in Table 3.

The potential energy of the ion Q with its image in the planar interface is²⁷

$$\Phi(x) = QQ' / 8\pi\epsilon_a(2x) = -Q^2(\epsilon_c - \epsilon_a) / 16\pi\epsilon_a(\epsilon_c + \epsilon_a)x. \quad (21)$$

Where the minus is a reminder that the potential is attractive. It is assumed that Boltzmann statistics apply so that the probability an isolated ion will be at a distance x from the interface ($2x$ from its image) is

$$P(x) \sim P(\infty) \exp(-W/kT) \quad (22)$$

with

$$W = - \int_{\infty}^x F(x) dx \quad \text{and} \quad F = QQ' / 4\pi\epsilon_0\kappa(2x)^2 \quad (22a)$$

where Q' is given by eqn (19). The ratio of particle densities $n(x)/n(\infty)$ may be equated to the probability ratio $P(x)/P(\infty)$ so that

$$n(x) \approx n(\infty) \exp \left[\frac{QQ'}{16\pi\epsilon_0\kappa_a x kT} \right], \quad (22b)$$

where $n(\infty)$ is the ion density in the amorphous region far from the interface. The density at the surface is $n(r_i)$ and the binding energy of an ion of radius r_i to the interface is

$$W(r_i, f) = \Phi(r_i, f) = -QQ' / 16\pi\epsilon_0\kappa_a r_i f \quad (23)$$

where f is near unity and is inserted into eqn (23) to represent departures of the interfacial region from an ideal mathematical plane. The number of molecular groups N_i (per unit volume) in eqn (20) is directly proportional to the density ρ . Thus by taking the ratio of eqn (20) for the crystalline and amorphous regions, a relation between κ_c , κ_a , ρ_c , and ρ_a is obtained,

$$\frac{\kappa_c - 1}{\kappa_c + 2} \cdot \frac{\kappa_a + 2}{\kappa_a - 1} \approx \frac{\rho_c}{\rho_a} \quad (24)$$

For present purposes of illustration it will be assumed that $\kappa_a \sim 3$ and $\kappa_c / \kappa_a \sim 1.1$. Thus eqn (20) gives $Q' \sim Q/59$ so that eqn (23) predicts an electrostatic binding energy $\Phi \sim 2.2 \times 10^{-2}$ eV for a monovalent ion of 1 Å radius. This is the same magnitude as kT at room temperature. A characteristic release of ions from such interfacial "traps" would be expected near a temperature

$$T_r \sim QQ' / 16\pi\epsilon_0\kappa_a r_i f k, \quad (25)$$

which might range from more than 400°K for small multivalent ions in a low dielectric constant polymer to less than 30°K for large monovalent ions in a polymer of high dielectric constant. It appears that some considera-

Table 3. Representative values of bond polarizabilities in SI-units†

Bond	C-C(al.)	C-C(aro.)	C=C	C-H(al.)	C-Cl	C=O	C≡N	N-H
$10^{30} \alpha_i [\text{m}^3]$	8.04	13.4	22.3	1.15	32.8	14.6	2.48	9.42

† $\alpha_{\text{SI}} = 4\pi \times 10^{-6} \alpha_{\text{cgs}}$, based on values quoted by J. O. Hirschfelder, C. F. Curtiss and R. B. Bird, *Molecular Theory of Gases and Liquids*, John Wiley, New York (1964). $\Delta\mu = \epsilon_0 \alpha \Delta\epsilon$.

tion should be given to these ideas in the analysis of data obtained by the methods of thermally stimulated currents, thermodepolarization, etc.

If the electrostatic interaction with a spherical interface of radius a is considered, the image charge is given by $Q' = -aQ/r$, where r is measured from the center of the sphere to the ion. The integration of the force is more complicated but the analysis can be made in a way that is analogous to the planar case.

D. The entropy correlation theory

Earlier in this paper the close connection between diffusion and ionic mobility has been noted. This connection can now be put to use to extend to the case of ionic mobility a theory that has been proposed by Barker, Tsai, and Willency²⁸⁻³⁰ and supported by extensive experiments involving gas diffusion in acrylic polymers. The study was undertaken to obtain a better understanding of the activation entropy ΔS^* which occurs in the rate theory usually associated with Eyring's name. When this rate theory is applied to diffusion the result for the diffusion coefficient can be expressed as the product of the specific rate k (1/sec) and the square of an average jump distance λ :

$$D = \lambda^2 k = \lambda^2 (k_B T / h) g \exp(-\Delta G^* / RT) \quad (26)$$

where the activation Gibbs' energy is

$$\Delta G^* = \Delta U^* + P\Delta V^* - T\Delta S^* \quad (27)$$

so that the parts of the experimentally determined diffusion equation, $D = D_0 \exp(-E_B^*/RT)$, can be identified with the activation energy (ΔU^*), volume (ΔV^*), and activation entropy (ΔS^*) portions of eqn (26).

Furthermore, the Nernst-Einstein-Townsend relation, $uk_B T = zeD$, enables one to obtain an expression for the mobility u and the conductivity σ in terms of the activation parameters. Thus for example

$$\sigma = nzeu = nz^2 e^2 (\lambda^2 k) / k_B T, \quad (29)$$

with

$$\sigma = \sigma_0 \exp(-\Delta U^* / kT), \quad (30)$$

and

$$\sigma_0 = (n\lambda^2 z^2 e^2 g / h) \exp(-1) \exp(\Delta S^* / R). \quad (31)$$

Our approach was to inquire: what will happen to ΔS^* if the polymer chain configurations are changed in a way that produces a known reduction in the configurational entropy ΔS_c ? The resultant theory that evolved is schematically illustrated in Fig. 4, and it may be stated as follows: When the configurational entropy S_c is reduced by an ordering process, such as stretching, an additional amount of local disorder must occur in the neighborhood of a diffusing molecule or ion before a unit diffusional process can take place. In other words

$$\Delta(\Delta S^*) = -\Delta S_c. \quad (32)$$

The increase in the activation entropy is equal to the decrease in the configuration entropy. Or, if Λ denotes an ordering parameter (in the experiments it was the elongation ratio) then

$$\Delta S^*(\Lambda) = \Delta S^*(1) - \Delta S_c. \quad (33)$$

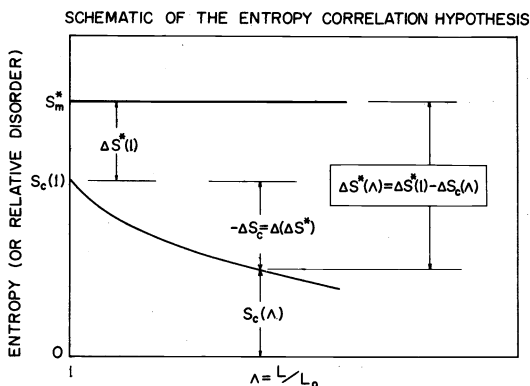


Fig. 4. Representation of the essential ideas of the entropy correlation theory.²⁹⁻³¹ The local disorder needed for an ion or molecule to make a diffusive step from one activated cluster of chain segments to another cluster corresponds to an entropy S_m^* . An ordering process (in this case uniaxial elongation) causes a change in the configurational entropy ΔS_c . In an experiment, the "observed" activation entropy is $\Delta S^*(1)$ before the ordering process and $\Delta S^*(\Lambda)$ after ordering.

The physical implication of the theory is that a certain minimal amount of disorder is needed in order for diffusion to occur and that this characterizes the activated state and is independent of the ordering parameter, thus giving the horizontal line S_m^* . If we specify the nature the ordering process, then ΔS_c will take on a special form. In our measurements up to this time we have used uniaxial elongation in the rubbery state followed by rapid quenching to freeze in configurational changes for which ΔS_c could be calculated using the theory of rubber elasticity. The analytical procedure is outlined in Fig. 5. Primary data for diffusion, or presumably for conduction, are treated by the rate theory formalism to give numerical values for the activation entropy ΔS^* as a function of Λ . The entropy correlation hypothesis is substituted into the rate theory expressions to give the general relation

$$\ln \frac{D_0(\Lambda)}{D_0(1)} = \ln \frac{\sigma_0(\Lambda)}{\sigma_0(1)} = -\frac{\Delta S_c}{R} + \text{w.f.g.} \quad (34)$$

where w.f.g. = $\ln [g(\Lambda)/g(1)]$ is a weak function of the geometrical parameter g . For the case studied experimentally, the relation from rubber elasticity theory for ΔS_c is

$$\Delta S_c = a_c [3 - \Lambda^2 - (2/\Lambda)] \quad (35)$$

so that the special version of the entropy correlation

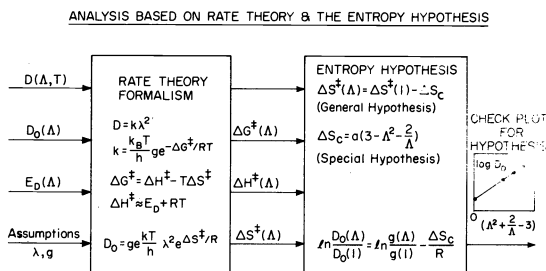


Fig. 5. Outline of an application of rate theory and the entropy correlation theory to diffusion measurements, illustrating the test plot for the correlation theory. $\log D_c$ can be replaced by $\log \sigma_0$, so far as known.

theory, that has been checked experimentally, corresponds to obtaining a straight line when $\ln [D_0(\lambda)/D_0(1)]$ is plotted against the function $\lambda^2 + (2/\lambda) - 3$. The results of measurements of the diffusion of CO, O₂ and N₂ in poly (isobutylmethacrylate) are shown in Fig. 6. Similar good agreement of theory and experiment has been found for many other pairs of gases and polymers.

E. The influence of moisture and dielectric constant on conductivity

The fact is well known that the presence of moisture can increase the observed level of conductivity by as much as 6 decades in some cases. Sharbaugh and Barker^{25,26} have explored the nature of the relationship between conductivity and dielectric constant for a long list of organic liquids for which measurements of both parameters on the same sample were available. Statistically there was a definite trend and by making suitable adaptations of the theory of weak electrolytes an equation was obtained to describe it. A qualitative explanation was given, of reasons for systematic deviations from the simple equation

$$\sigma \approx c_w^{1/2} 10^{-4.34} 10^{-20.8/\kappa'} \quad (36)$$

or

$$\sigma \approx c_w^{1/2} e^{-10} e^{-47.9/\kappa'} \quad (37)$$

where σ has the unit $\Omega^{-1} \text{cm}^{-1}$ when the water concentration C_w is expressed in moles/liter. The constants were obtained by treating some measurements of σ and κ' as functions of concentrations for mixtures of water and dioxane. Ionic conduction in a polymer occurs when ionizable groups present as part of the macromolecule or as impurities dissociate and thus provide a dynamic equilibrium of mobile ions. Thus the essential ideas of the work by Sharbaugh and Barker²⁶ are that water modifies the conductivity by (1) partial dissociation to mobile ions and (2) by increasing the effective dielectric constant of the system, thus enhancing dissociation of ionically bound groups present within the polymer. The solubility limit of water in the polymer influences the correlation. Using calculations analogous to the methods discussed by Debye³¹ it can be seen that when water ($\kappa'_w = 78$) is added to a typical non-polar polymer ($\kappa'_p \approx 2.5$) the effective dielectric constant of the mixed system (κ') changes very little until the water concentration exceeds about 1 wt%.

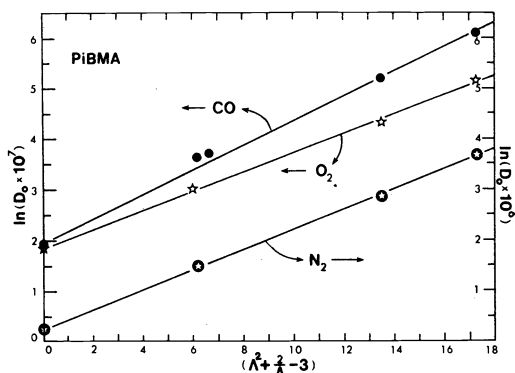


Fig. 6. Test plot for the entropy correlation theory applied to diffusion data of Tsai,²⁹ for nitrogen, oxygen, and carbon monoxide in poly(isobutyl methacrylate).

However, even parts per million of absorbed water can cause substantial increases in conductivity. Therefore, at low water concentrations, the dissociation of H₂O is the important effect, whereas at higher concentrations enhanced dissociation of all ionic species becomes important. Figure 7 gives some data compiled by Sasabe,³² plotted to show the correlation with eqn (36) for several values of water concentration. It should be noted that the upper most curve for $c_w = 10^{-8}$ mol/l corresponds to only 6×10^{12} molecules/cm³ and that presumably only a small fraction of these dissociate. It also is significant to note that in several cases two or more modifications of the same polymer are given, for example points 27, 27', and 27'' are respectively for dry and moist samples of cyanoethylated cellulose, similarly 19 and 19' are for dry and moist polyurethane, 12 and 12' are for polyvinyl chloride and plasticized PVC, and the dashed curves on the left are for cellulose acetate doped with RbCl and CaCl₂ from the data of Barker and Thomas.³³ In most cases the curves for the individual materials are steeper than the curves that correlate the trend for the ensemble of materials. As a qualitative explanation for this effect, it is thought that a very dry and pure polymer of some particular dielectric constant, say 3 for example, would have a very low conductivity, perhaps less than $10^{-20} \Omega^{-1} \text{cm}^{-1}$ but as trace water is added σ would rise along an almost vertical line because the small amount of water would have little effect on the dielectric constant. However, if more water were sorbed the curve would begin to bend toward the left axis, perhaps passing near points 12, 15, and 21. In most low dielectric constant organic substances, there is a relatively limited solubility for water so when this point is reached the upper limit for conductivity by this water dissociation mechanism would have been reached. The level of other impurity ions would make perhaps an order of magnitude difference in the maximum conductivity. Thus the position of a given polymer on Fig. 7 has an upper bound of $\log \sigma$ that is determined by the limit of water solubility in the material and by the dissociation of the set of ionic groups present.

LOG (DC-CONDUCTIVITY) VS RECIPROCAL DIELECTRIC CONSTANT ϵ' (100 Hz) FOR POLYMERS AT 25°C.

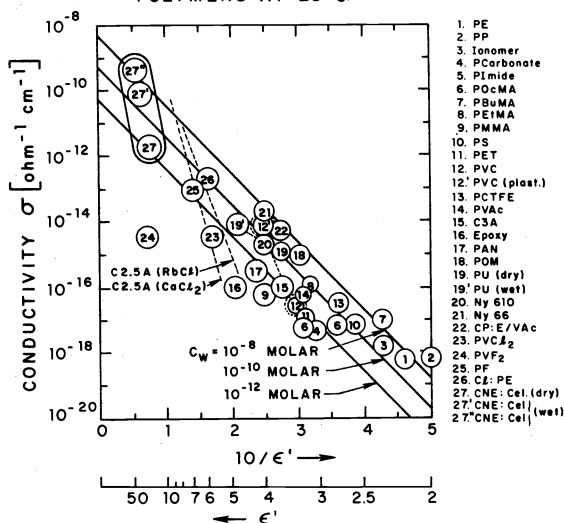
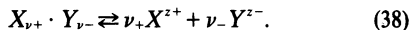


Fig. 7. Comparison of the Sharbaugh-Barker relation (eqn (36)) with data assembled by Sasabe.³² The correlation is taken as evidence of ionic rather than electronic processes.

There is a fairly weak dependence on salt concentration, such that $\log \sigma$ is proportional to²⁶

$$-(\nu_+ + \nu_- - 1)/(\nu_+ + \nu_-) \log C_{\text{salt}}$$

where the ν 's are stoichiometric numbers in the reaction



The lower bound would be determined by statistical factors related to trace water content.

4. SELECTED METHODS OF INVESTIGATION

In this section a few of the many possible additional techniques for determining the characteristics of ionic conduction in polymers are discussed. Only two will be discussed in much detail. This reflects more of a limitation of time and space than of a ranking of techniques by importance. The alternating current technique was chosen for detailed treatment because it provides some information not readily available by direct current methods and enables one to avoid some of the problems that direct current methods lead one into, for example polarization by space charge build up.

A. Non-ohmic high field behavior

Non-ohmic processes have played such an important role in semi-conductor physics that there is a tendency to interpret the occurrence of a non-linear current-voltage characteristic as prima facie evidence for an electronic conduction mechanism.

This of course is not the case because there are many factors that can lead to non-ohmic behavior in polymers. Some of these are given in Fig. 8 along with some reasons for similar behavior in electronic semi-conductors. The vertical order is meant to be a crude assessment of their

POSSIBLE SOURCES OF NON-OHMIC CONDUCTION

(IONIC)	(IONIC & ELECTRONIC)	(ELECTRONIC)
① COMBINATION OF OTHERS		
② BIASED DIFFUSION OVER BARRIERS (STERN-EYRING)	④ FIELD EMISSION FROM CONDUCTORS (SCHOTTKY, RICHARDSON)	
③ FIELD-ENHANCED DISSOCIATION (ONSAGER)	⑤ FIELD-ENHANCED DETRAPPING OF e ^s (POOLE-FRENKEL)	
⑥ SPACE CHARGE LIMITED (CHILDS)		
⑦ LOCAL STRUCTURE INFLUENCED BY ELECTRIC FIELD	⑧ QUANTUM TUNNELING THRU BARRIERS (FOWLER-NORDHEIM)	
⑨ CHEMICAL REACTIONS AT ELECTRODES		
⑩ INTERNAL OHMIC HEATING (j^2/σ)		
⑪ VON HIPPLE'S PHOTON EXCITATION	⑫ OTHER QUANTUM EFFECTS	

Fig. 8. Outline of possible sources of non-ohmic conduction.

relative probability of having produced non-ohmic behavior in a given case. Obviously item 1 is the most likely because it includes the others. When two or more of these processes occur together it makes the dilemma of ionic vs electronic more difficult to unravel. Space charge can cause very large departures of the local field intensity from the mean value V/b , so that the local field near an electrode might in fact be large enough to produce a significant Schottky effect whereas a field of the average value would not. Internal heating due to the j^2/σ power dissipation per unit volume is an often overlooked source of apparent non-ohmic behavior. It can result in an increase in the internal temperature of a sample even though the surfaces are maintained at constant temperature.

Some of the electronic non-ohmic processes are summarized in more detail in Fig. 9. The equations are written as J/E to be equivalent to a conductivity. It should

Non-ohmic electronic processes

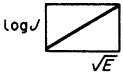
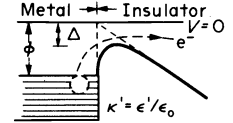
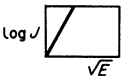
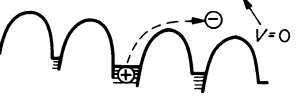
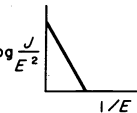
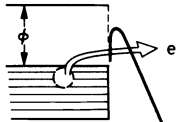
Name of effect and usual test plot	Descriptive equations	Physical interpretation
Schottky-(Richardson) emission 	$\frac{J}{E} = \frac{A_R T^2}{E} \exp \left[\frac{B_S E^{1/2} \phi}{kT} \right]$ $A_R = 1.2 (10^6 \text{ A/m}^2)$ $B_S/k = 0.44 / \sqrt{\kappa'}$	 Field assisted hopping over image barrier at cathode
Poole-Frenkel effect 	$\frac{J}{E} = A_R T^2 E^{-1} \exp \left[\frac{B_P E^{1/2} - \phi}{kT} \right]$ $A_R = 1.2 (10^6 \text{ A/m}^2)$ $B_P/k = 0.88 / \sqrt{\kappa'}$ $B_P = 2 B_S$	 Field assisted electron-hole separation within bulk of sample
Fowler-Nordheim emission 	$\frac{J}{E} = 1.54 (10^{-6}) \frac{E}{\phi} \exp \left[\frac{-6.8}{(10^{-9})} \frac{\phi^{3/2}}{E} \right]$ (No explicit dependence on temperature)	 Quantum tunneling through image barrier

Fig. 9. Interpretations, equations, and typical test plots for three important non-ohmic electronic processes.

be noted that the Schottky–Richardson and the Poole–Frenkel^{34–36} effects have very similar equations and test plots. In both cases $\log j$ vs $E^{1/2}$ should be linear, however the slope for the Poole–Frenkel case, which involves electron-hole separation within the bulk is twice the slope for the Schottky case which is due to the lowering of the surface potential barrier by an applied field. It seems reasonable to suppose that the Poole–Frenkel and Schottky–Richardson effects could occur simultaneously, in which case an intermediate slope-or a region of transition from one slope to the other might occur. If a very much larger field is applied than in the Schottky case, the potential barrier will become sufficiently thin that electron tunneling can occur. This is called Fowler–Nordheim emission is not explicitly dependent on temperature.⁷ The test plot is a linear dependence $\log (J/E^2)$ on $1/E$.

Figure 10 illustrates three of the important sources of non-ohmic behavior in ionic conductors. In the rate theory, an ion has less of a barrier to diffuse over in the direction of the field than in the opposite direction. The field dependent mobility

$$u = \frac{Dq}{kt} \left[\frac{e^{aw} - e^{(\alpha-1)w}}{w} \right] \quad (39)$$

is in the generalized form discussed by Barker and Thomas³³ where w is a dimensionless field intensity $Eq\lambda/kT$ and α is an asymmetry parameter defined as the ratio of though-to-peak forward jump distance to the total jump distance λ . If the energy function is symmetrical, $\alpha = 1/2$ and eqn (39) reduces to the more familiar form

$$u = (2Dq/kT w) \sinh (w/2). \quad (40)$$

A small amount of asymmetry could make a significant

difference in the results. The evidence for or against asymmetry is not conclusive. The most frequently used test plot appears to be the one used by Amborski.¹⁰ It consists of a plot of $\log j$ vs E which asymptotically approaches a straight line whose slope is $(q\lambda/4.6kT)$ decades per unit of E . For my own use I prefer, as in Fig. 11, to plot $\log \sigma$ (or $\log I/V$) vs $\log E$ (or $\log V$) because such a plot appears to be more sensitive to the precision of the data and shows Ohm's law as a horizontal line.

The Onsager³⁸ theory of field retarded recombination produces an upward swing in current vs voltage that is qualitatively similar to the rate theory expression but when examined in detail, it has a somewhat different shape in the region where the non-ohmic behavior first begins to be experimentally apparent. The theory has

COMPARISON OF THEORY & EXPERIMENT FOR POLYCARBONATE

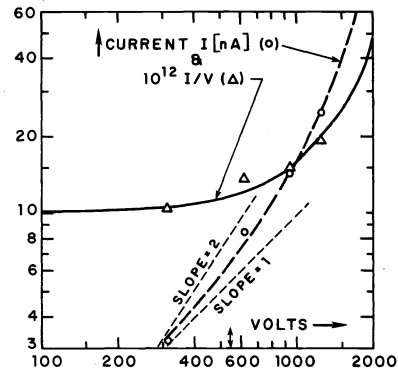


Fig. 11. Comparison of the modified rate theory³³ with non-ohmic data by Marshall³⁹ for poly(bisphenol-A carbonate). Ohm's law is a horizontal straight line for the plot of I/V vs V (triangles).

Non-ohmic ionic processes

Name of effect and typical test plot	Descriptive equations	Physical interpretation
Modified Stern-Eyring rate theory 	$\sigma = \frac{J}{E} = nuq$ $u = \frac{Dq}{kT} \left[\frac{e^{aw} - e^{(\alpha-1)w}}{w} \right]$ $w = Eq\lambda / kT$	
Onsager theory 	$\frac{\sigma(E)}{\sigma(0)} = \left\{ \frac{2iJ_1(if)}{f} \right\}^{1/2}$ $f = 88.1T\sqrt{E/\kappa}$ $E \text{ in [V/m]}$	
Space-charge-limited conduction 	$\text{If } v = uE, \frac{J}{E} = \frac{9}{8} \epsilon_0 u \frac{V}{b^2}$ $\text{If } v = \sqrt{\frac{2eV}{m}}, \frac{J}{E} = \frac{4}{9} \epsilon_0 \left(\frac{2e}{m}\right)^{1/2} \frac{V^{1/2}}{b}$	

Fig. 10. Interpretations, equations, and typical test plots for three important non-ohmic ionic processes. The $\log \sigma$ vs E ($\sigma \log (I/V)$ vs V) plots is in some respects preferable for the rate theory also. There are many other relations for space charge.¹

fewer free parameters than the rate theory so it is a bit easier to see whether or not it fits.

Space charge limited conduction can take many forms depending on details of the geometry, boundary conditions, and whether the ions are free to accelerate between collisions, or whether they dissipate energy virtually continuously. One typical effect of the space charge is to reduce the field intensity on the interior of a sample and increase it near the electrodes. Guttman and Lyons¹ list twelve different functions for calculating space charge limited currents in different situations in semiconductors. The data for polycarbonate shown in Fig. 11 were taken by Marshall³¹ they are compared with the rate theory for symmetrical barriers ($\alpha = 1/2$). The fit is seen to be quite reasonable. Another advantage of the log-log plot for this kind of comparison is that the curve for I/V vs V and for j/E vs V will be identical in shape. The best fit is obtained by parallel translation of a master curve. A previously unpublished analysis of some data of Thomas and Barker³³ is shown in Fig. 12, with RbCl-doped-cellulose 2.5 acetate for the top pair of curves and an undoped reference sample for the bottom curve. On the I/V plots it appears that the rate theory gives a much better fit than the Onsager theory. The best fit (RbCl) was obtained by matching the point $w = \lambda qE/kT = 1$ of the master curve with the point $V = 250$ volts on the graph. The sample was at 300°K and its thickness b was 270 μm so that $\lambda = kTb/qV \approx 280 \text{ \AA}$. If a very literal interpretation of the rate theory is taken, then ions will not on the average be closer together than the spacing between potential minima so that as an upper limit for the concentration

$$n_{U.L.} \sim (1/\lambda)^3 \sim 4.5 \times 10^{22} \text{ ions/m}^3.$$

The salt content n_0 , on the basis of X-ray techniques³⁹ is

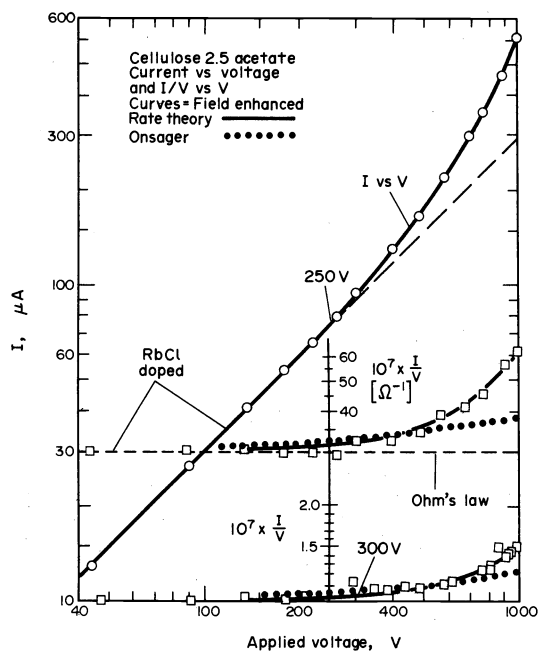


Fig. 12. Comparison of rate theory (solid curves) and Onsager's³⁸ theory (dotted curves) with data for cellulose 2.5 acetate that had been soaked in 0.1 molar RbCl for 48 hr.³⁹ The data at the lower right are I/V for a comparison sample of C2.5A which was soaked in distilled water for 48 hr. Thickness 279 μm area 19 cm^2 , temperature 24°C.

estimated to have been 4.7×10^{24} molecules/ m^3 and thus an upper limit for the fractional dissociation $\phi_{U.L.}$ is

$$\phi_{U.L.} \sim n_{U.L.}/n_0 \sim 1\%.$$

Correspondingly, the lower limit for the mobility with $\sigma \sim 4 \times 10^{-7}$ rom is

$$u_{LL} \sim \sigma/en_{U.L.} \sim 5 \times 10^{-13} \text{ m}^2/\text{V sec}.$$

It is of interest to note that the "jump distances" in the rate theory are of the same magnitude as the "domain" size discussed in conjunction with eqn (16) and Fig. 2.

Before leaving the subject of non-ohmic behavior, it should be informative to examine the comparison of the rate theory with the Schottky and Poole-Frenkel plot ($\log I$ vs $V^{1/2}$) shown in Fig. 13. The circles were taken directly from a plot of the theoretical master curve for the rate theory. I recently tricked a very competent scientist friend who thought he was looking at a plot of experimental data into saying the plot looked like evidence for an electronic Poole-Frenkel process to him. The triangles are plotted from a theoretical Fowler-Nordheim curve and also turn out to appear as a straight line over this small range of $V^{1/2}$. The reader may draw his own conclusions.

B. An alternating current technique

It is known in servomechanism theory and in circuit design engineering that almost any relatively smooth frequency response curve can be matched by some combination of resistors and capacitors, i.e. by an RC-network. Von Hippel⁴⁰ has given some good examples. The current in an ideal capacitor C will lead the sinusoidal voltage $V = V_0 e^{j\omega t}$ by 90° in phase, but the

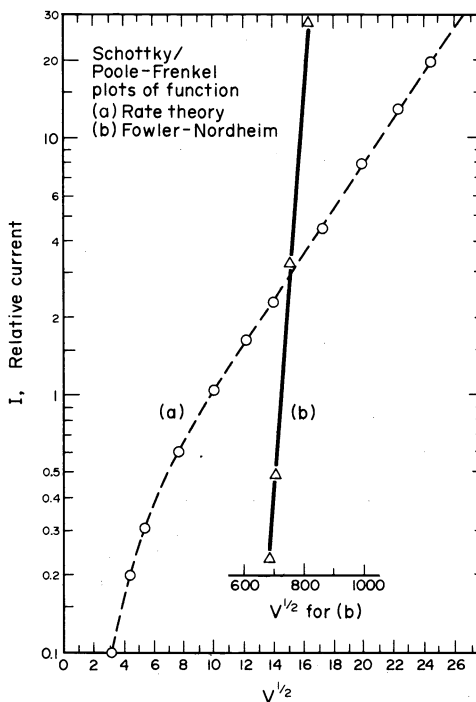


Fig. 13. Plots of (a) rate theory and (b) Fowler-Nordheim theory on the Schottky/Poole-Frenkel test plot ($\log I$ vs $V^{1/2}$). Some researchers interpret long linear sections on such plots as evidence for electronic conduction processes.

current and voltage are in phase in an ideal resistor R . As illustrated in Fig. 14, the component admittances in a parallel RC-combination add to give a total admittance (reciprocal impedance) $Y = j\omega\kappa^*C_0$ where $j = \sqrt{-1}$, $\kappa^* = \epsilon^*/\epsilon_0$, ω is the angular frequency, and C_0 is the capacitance the capacitor would have if the static dielectric constant κ_0 were unity. Due to the relation $\kappa^* = \kappa' - j\kappa''$ the results for the equivalent circuits can be expressed directly in terms of the real and imaginary parts of the dielectric constant and the loss tangent, $\tan \delta$ can be calculated from κ''/κ' . By identification with related terms in expressions based on molecular models of dielectrics due to Debye and others,³¹ the series RC-circuit corresponds to a polar dielectric with viscous relaxation of the dipoles and the parallel RC-circuit, to a dielectric with ohmic or conductive losses. This provides the basis for a neat way to separate ionic conduction currents from the Maxwell displacement currents in a.c. measurements. The most significant thing to note in the results for the equivalent circuits is that for a parallel RC-circuit, $\log(\tan \delta)$ vs $\log(\omega)$ would be linear of slope minus one and for a series RC-circuit the slope would be plus one. By combining the parallel and series RC-elements reasonable fits can be obtained over surprising wide ranges of data. The examples in the figure are for water and Pyranol (a General Electric Company mixture of isomeric pentachlorodiphenyls known for its good low frequency properties). Note how the $\tan \delta$ curves, near 10^6 Hz, cross at almost a right angle. This corresponds to the fact that water has a large amount of ionic conduction whereas Pyranol's behavior is dominated by the viscous relaxation of polar molecules.

Reed⁴¹ has made good use of the equivalent circuit technique to study the effects of impurities on the ionic conductivity of poly(2,6-dimethyl-1,4-phenylene ether), which has the General Electric trademark PPO. His analysis is a bit more involved than the preceding discussion of water might lead one to believe and Fig. 15 is included to illustrate his method and summarize the result. The (a) part shows a $\log(\tan \delta)$ vs $\log f$ plot and the

dashed line has the slope of minus one, to be expected for ionic conductivity. Ionic conduction appears to be present but partially obscured by at least two other loss mechanisms related mainly to dipole motions. To separate

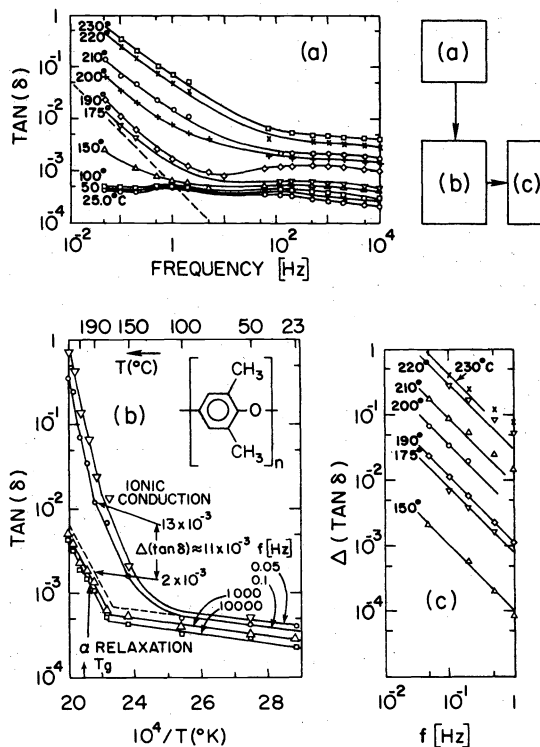


Fig. 15. Reed's⁴¹ application of alternating voltage techniques to obtain the ionic conduction losses at low frequencies in the presence of a large dipolar background. (a) is the original data, (b) is an extrapolation procedure to obtain the background, and (c) is the resultant loss due to ions after the subtraction in (b). The polymer was poly(2,6-dimethyl 1,4-phenylene ether), 22000 ± 3000 g/mol, 440 μm thick, with gold electrodes of 4 cm diameter.

EQUIVALENT CIRCUIT	ANALYSIS FOR SINUSOIDAL V	RESULTS
<p>PARALLEL</p> <p>$\tau = RC$</p>	<p>CURRENTS ADD (OR ADMITTANCES ADD)</p> $I = \frac{V}{R} + C \frac{dV}{dt}$ $Y = 1/Z = I/V = 1/R + j\omega C$ <p>BUT $Y = j\kappa^*\omega C_0 = (\kappa'' + j\kappa')\omega C_0$</p>	<p>$\kappa' = \frac{C}{C_0}$</p> <p>$\kappa'' = \frac{C''}{\omega RC}$</p> <p>$\tan \delta = \frac{C''}{\omega RC}$</p>
<p>SERIES</p> <p>$\tau = RC$</p>	<p>VOLTAGES ADD (OR IMPEDANCES ADD)</p> $V = IR + 1/C \int_0^t I dt$ $Z = V/I = R - j/\omega C = 1/Y$	<p>$\kappa' = \frac{C}{C_0}$</p> <p>$\kappa'' = \frac{C''}{\omega RC}$</p> <p>$\tan \delta = \frac{\omega RC C''}{1 + (\omega RC)^2}$</p>
<p>COMBINATION</p> <p>$\tau_1 = R_1 C_1$ $\tau_2 = R_2 C_2$</p> <p>PYRANOL $R_1 \approx \infty$ $R_2 = 47 \Omega$ $C_1 = 2.7 \text{ nF}$ $C_2 = 2.3 \text{ nF}$</p> <p>WATER 53000Ω 0.085Ω 0 100 pF</p>	$Y = \frac{1}{R_1} + j\omega C_1 + \frac{1}{R_2 - j/\omega C_2}$ $\kappa' = \frac{C_1}{C_0} + \frac{(C_2/C_0)}{1 + \omega^2 \tau_2^2}$ $\kappa'' = \frac{(C_2/C_0)\omega \tau_2}{1 + (\omega \tau_2)^2} + \frac{1}{R_1 C_0 \omega}$	<p>5 4 3 2 1 0</p> <p>10⁴ 10⁶ 10⁸ 10¹⁰</p> <p>TAN δ</p> <p>FREQUENCY [Hz]</p> <p>--- CIRCUIT — DATA</p>

Fig. 14. Outline of the use of RC-circuit elements to match the electrical frequency response of a material. In particular note the results for $\tan \delta$.

the background of dipolar losses from the conduction loss, the idea that dipolar motions are thermally activated was used. Thus the information in (a) was cross plotted in an Arrhenius diagram in (b) and the expected linear segments at high frequencies were used as a basis to extrapolate the dipolar part of the low frequency curves. Only one extrapolated curve is shown (dashed, for 0.1 Hz). Then as illustrated for 190°C the dipolar background (in this case $(\tan \delta)_d \sim 2 \times 10^{-3}$) is subtracted from the total $\tan \delta (12 \times 10^{-3})$ to give $\Delta(\tan \delta) = (\tan \delta)_i$, the part due to conduction. Part (c) then shows the plot to check the method and display the losses due to conduction. The equivalent circuit model also enables one to determine the conductivity from the sample dimensions and its conductance.

$$G_x = 2\pi f C_x \tan \delta. \quad (41)$$

Reed found that the activation energies were about 43 ± 2 kcal/mol above T_g ; 22.5 ± 5 kcal/mol below T_g . These values are consistent with those found for side group and short chain segment movements below T_g and for the large scale α -relaxation of long segments above T_g so it appears that the ions respond to the polymer molecules' motions as one expects. By carefully purifying the polymer through a series of procedures and then measuring the nitrogen and copper content, Reed's study provides much more quantitative information than is typically available for systems of this type. In fact by utilizing the data given in his Table, I have been able to infer that the contribution to the conductive loss due to the residual amine catalyst was 5×10^{-6} per ppm of N and that the loss contribution due to the copper salt present was 42×10^{-6} per ppm of Cu. The deduction of the amine contribution was obtained in a straight forward way by plotting $(\tan \delta)_c$ vs Reed's values for nitrogen concentration and is shown in Fig. 16(a). However since there were orders of magnitude more amine than copper, it was necessary to first subtract the amine contribution, L_N , to $\tan \delta$. This was done by taking L_N as the product of the amine slope (5×10^{-6} /ppm-N) times the amine concentration [N]. The results are shown in Fig. 16(b).

Another simple but powerful technique, to which the ac analysis could be applied, is one developed by Devins.⁴² Rather than using Reed's approach of a series of purifications followed by trace analysis of residual impurities, Devins added relatively large known amounts of acetic acid to the polymer (polycarbonate) and then measured $\tan \delta$ vs frequency, temperature, and acetic acid content. A rationale is that the acetic acid is a model compound for ionizable impurities and that by extrapola-

tion to zero concentration one can infer much about ionic and dielectric interactions in such systems.

Very recently Reich and Michaeli^{43,44} also have utilized a.c. techniques and have shown that it can be helpful to analyze dielectric data in terms of the "dielectric modulus" $M^* = 1/\epsilon^*$. Their work has an additional special interest because of the large quantities of pseudo-free ions they were able to incorporate by polymerizing solutions of mono- and multivalent salts in liquid monomer.

C. Other important techniques

There is an impressive array of other techniques for studying ions in polymers. Space does not allow for the discussion they deserve but two must be mentioned: (1) the use of hydrostatic pressure and (2) thermally stimulated currents and related methods.

The work of Sasabe *et al.*^{12,13} shows the excellent results that can be obtained by using hydrostatic pressure as an additional variable. In essence the ionic conductivity decreases as pressure is applied such that $\log \sigma$ vs p has linear sections that join in a region of pressure that can be called the glass transition pressure p_g , which depends on temperature. The slopes of the $\log \sigma$ vs p curves give activation volumes

$$\Delta V^* = -RT(\partial \ln \sigma / \partial p)_T \quad (42)$$

which, being typically over $100 \text{ cm}^3/\text{mol}$ in the rubber state and somewhat less than that in the glass, suggest the involvement of a considerable number of units of the polymer molecule in the activation process. For Nylon 66, they found ΔV^* (rubber) = $72 \text{ cm}^3/\text{mol}$ and ΔV^* (glass) = $58 \text{ cm}^3/\text{mol}$. These positive values are more suggestive of ionic conduction than of electronic, where the usual but not exclusive case is to obtain negative activation volumes.

Thermal techniques for studying the electrical properties of polymers are useful and currently are enjoying considerable popularity. There are numerous variants of two main types of experiments. In one type, the sample is cooled, exposed to ionizing radiation of some kind, and then current i is measured as the sample warms with an electric field applied. Peaks in the i vs T curves are used to estimate the depth of traps for the charge carriers. The other technique is more recent and involves quenching a heated sample in a strong electric field. Then the field is removed and current (or voltage) is observed as the sample is heated again. To see what scope and detail of information may be obtained the series of interesting papers by Pfister *et al.*⁴⁵⁻⁴⁷ can be consulted. Here too, there are sometimes questions of whether ionic space charges, or rotating dipoles, or trapped electrons cause a given observed effect. See also the work by Murayama.⁴⁸

5. CONCLUSION

The presence of mobile ions in solid polymers creates an array of problems that are of both academic and technological interest. Since such ions contribute to dielectric losses at low frequencies their presence is sometimes undesirable in capacitors for example, but in many other cases their presence is the basis for technological application, such as for ion exchange membranes or for certain graded high-voltage insulators. The discussion of the local structure hypothesis makes it evident that an ion has a rather large domain of influence and that the principle that an ion will try to relocate itself

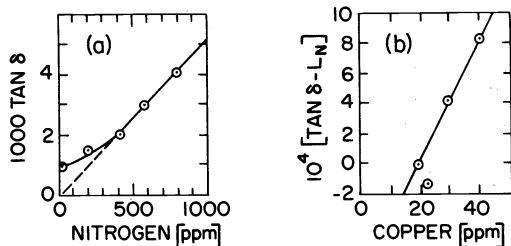


Fig. 16. Calculations, based on the data of Reed,⁴¹ of the contribution to dielectric loss due to ions in the polymer (see Fig. 16). "Nitrogen" refers to the concentration of N in amine salts formed from residual catalyst (800 ppm = 1 N per chain). "Copper" also is from residual copper salt catalyst.

to minimize its Gibbs' free energy has many important implications. For example, if not otherwise impeded, an ion will migrate from a region of low dielectric constant to a place where κ is larger. Thus, in anthropomorphic terms, an ion would prefer electrostatically to be inside of a crystallite rather than in the amorphous material outside but the mechanical energy required to create the vacant space in the crystallite opposes the electrostatic driving force and the ion is likely to compromise by attaching itself to the interface. This same principle can be used to better understand how ions can get inside of a polymer to begin with and why moisture has some of the effects it does.

With the wide array of techniques now available to study ionic conduction in polymers much progress should be in store and perhaps many of the dilemmas can be resolved.

REFERENCES

- ¹F. Gutmann and L. E. Lyons, *Organic Semiconductors*. John Wiley, New York (1967).
- ²H. F. Mark, *Am. Chem. Soc. Polym. Prep.* **16**, 764 (1975).
- ³F. J. Norton, *J. Appl. Polym. Sci.* **7**, 1694 (1963).
- ⁴A. E. Binks and A. Sharples, *J. Polym. Sci. A2*, **6**, 407 (1968).
- ⁵D. A. Seanor, *J. Polym. Sci. A2*, **6**, 463 (1968).
- ⁶D. D. Eley and D. I. Spivey, *Trans. Faraday Soc.* **57**, 2280 (1961).
- ⁷G. King and J. A. Medley, *J. Colloid Sci.* **4**, 1 (1949).
- ⁸A. J. Murphy, *Can. J. Phys.* **41**, 1022 (1963).
- ⁹M. Ieda, G. Sawa, S. Nakamura and Y. Nishio, *J. Appl. Phys.* **46**, 2796 (1975).
- ¹⁰L. E. Amborski, *J. Polym. Sci.* **62**, 331 (1962).
- ¹¹Y. Inuishi and D. A. Power, *J. Appl. Phys.* **28**, 1017 (1957).
- ¹²S. Saito, H. Sasabe, T. Nakajima and K. Yoda, *J. Polym. Sci. A2*, **6**, 1297 (1968).
- ¹³H. Sasabe, K. Sawamira, S. Saito and K. Yoda, *Polym. J.* **2**, 518 (1971).
- ¹⁴E. Sacher, *J. Macromol. Sci. Phys.* **4**, 441 (1970).
- ¹⁵D. Kiessling and B. Muendoerfer, *Plaste. Kaut.* **16**, 348 (1969).
- ¹⁶G. Lengyel, *J. Appl. Phys.* **37**, 807 (1966).
- ¹⁷A. C. Lilly, Jr. and J. R. McDowell, *J. Appl. Phys.* **39**, 141 (1968).
- ¹⁸D. M. Taylor and T. J. Lewis, *J. Phys.* **D4**, 1346 (1971).
- ¹⁹F. S. Smith and C. Scott, *Brit. J. Appl. Phys.* **17**, 1149 (1966).
- ²⁰R. A. Robinson and R. H. Stokes, *Electrolyte Solutions*. 2nd Edn, Butterworth, London (1959).
- ²¹R. A. Foss and W. Dannhauser, *J. Appl. Poly. Sci.* **7**, 1015 (1963).
- ²²J. E. Scheirer and W. Dannhauser, 1973 Annual Report Conf. on El. Insul. and Del. Phen. (Natl. Acad. Sci. Publ. IBSN 0-309-02229-0, p. 105 (1974).
- ²³J. H. Kallweit, *J. Polym. Sci. A1*, **4**, 337 (1966).
- ²⁴R. E. Barker, Jr. and C. R. Thomas, *J. Appl. Phys.* **35**, 87 (1964).
- ²⁵R. E. Barker, Jr. and A. H. Sharbaugh, *J. Polym. Sci. C10*, 139 (1965).
- ²⁶A. H. Sharbaugh and R. E. Barker, Jr. in *Phénomènes de Conduction dans les Liquides Isolants*. Edition du Centre National de La Recherche Scientifique, Paris, No. 179, 349 (1970).
- ²⁷J. J. Thompson, *Elements of the Mathematical Theory of Electricity and Magnetism* 5th Edn, p. 125, Cambridge University Press (1921).
- ²⁸R. A. Willency, M. S. Thesis in Materials Science, University of Virginia (Aug. 1970).
- ²⁹R. C. Tsai, Ph.D. Dissertation in Materials Science, University of Virginia (Mar. 1973).
- ³⁰R. E. Barker, Jr., P. S. Marshall and R. C. Tsai, 1971 *Ann. Rept. Conf. Elec. Insul. Dielectr. Phenom.*, Natl. Acad. Sci., Publ. No. 2032 65 (1972).
- ³¹P. Debye, *Polar Molecules* (Chemical Catalog Co. New York), Dover, New York (1929).
- ³²H. Sasabe, Researches of the ElectroTechnical Laboratory No. 721, Agency of Industrial Sci. and Tech., Tokyo (Dec. 1971).
- ³³R. E. Barker, Jr. and C. R. Thomas, *J. Appl. Phys.* **35**, 3203 (1964).
- ³⁴B. Swaroop, 1970 *Ann. Rept. Conf. Electr. Insul. Dielectr. Phenom.* Natl. Acad. Sci. Publ. No. 1870, 165 (1971).
- ³⁵J. J. O'Dwyer, *J. Appl. Phys.* **37**, 599 (1966).
- ³⁶P. L. Young, *J. Appl. Phys.* **46**, 2794 (1975).
- ³⁷W. R. Harper, *Contact Electrification* p. 126, Clarendon Press, London (1967).
- ³⁸L. Onsager, *J. Chem. Phys.* **2**, 599 (1934).
- ³⁹C. R. Thomas and R. E. Barker, Jr., *J. Appl. Polym. Sci.* **7**, 1933 (1963).
- ⁴⁰A. von Hippel, *Dielectrics and Waves*. p. 86. John Wiley, New York (1954).
- ⁴¹C. W. Reed, In *Dielectric Properties of Polymers*, (Edited by F. E. Karasz), p. 343. Plenum Press, New York (1972).
- ⁴²J. C. Devins, 1968 *Ann. Rept. Conf. Electr. Insul. Dielectr. Phenom.*, Natl. Aca. Sci. Publ. No. 1705 121 (1969).
- ⁴³S. Reich and I. Michaeli, *J. Polym. Sci., Polym. Phys. Ed.* **13**, 9 (1975).
- ⁴⁴S. Reich and I. Michaeli, *Abstracts, Int. Symp. Macromolecules*, Jerusalem (1975).
- ⁴⁵G. Pfister, M. A. Abkowitz and R. G. Crystal, *J. Appl. Phys.* **44**, 2064 (1973).
- ⁴⁶G. Pfister and M. A. Abkowitz, *J. Appl. Phys.* **45**, 1001 (1974).
- ⁴⁷M. A. Abkowitz and G. Pfister, *J. Appl. Phys.* **46**, 2559 (1975).
- ⁴⁸N. Murayama, *J. Polym. Sci.: Polym. Phys. Ed.* **13**, 929 (1975).
- ⁴⁹M. M. Labes, Abstracts, This Meeting, p. 205.